Angular-dependent metal-enhanced fluorescence from silver colloid-deposited films: opportunity for angular-ratiometric surface assays†‡

Kadir Aslan, Stuart N. Malyn and Chris D. Geddes*

Received 18th June 2007, Accepted 14th August 2007
First published as an Advance Article on the web 23rd August 2007
DOI: 10.1039/b709170b

We describe an exciting opportunity for Metal-Enhanced Fluorescence (MEF)-based surface assays using an angular-ratiometric approach to the observed enhanced emission from fluorophores in close proximity to silver colloids deposited on glass substrates. This approach utilizes the radiationless energy transfer (coupling) between the excited states of the fluorophore and the induced surface plasmons of the silver colloids, and the subsequent angular-dependent fluorescence emission from the fluorophore–silver colloid system. Since MEF is related to surface plasmons' ability to scatter light, angular-dependent light scattering from three different silvered surfaces and glass substrates were investigated using two common excitation angles, 45 and 90°. The scattered light from silvered surfaces with a high loading was observed at wider angles on both sides of the glass substrates, while forward scattering (from the back of the glass) was dominant for the silvered surfaces with low loading, as explained by both Mie and Rayleigh theories. When silver colloids were placed between the fluorophore and glass interface, the coupled fluorescence emission through the higher refractive index glass (and in air), increased in an angular-dependent fashion, following closely the angular-dependent light scattering pattern of the silver colloids themselves. Similar observations for fluorescence emission from fluorophores deposited onto glass surfaces alone were made, but at much narrower angles on both sides of the fluorophore–glass interface and were simply explained by Lambert's cosine law. As the loading of silver on glass was increased, the enhanced fluorescence emission was observed at wider angles (towards 0 and 180°) at both sides of the silvered surfaces. Glass surfaces without silver colloids were used as control samples to demonstrate the benefits of MEF for enhancing fluorescence signatures in an elegant, angular-dependent fashion. Finally, the utility of the angular-dependent MEF phenomenon for intensity-based angular-ratiometric surface assays is demonstrated.

Introduction

Metal-Enhanced Fluorescence (MEF) is a phenomenon where the quantum yield and photostability of fluorescing species in close proximity to metallic nanoparticles are dramatically increased.[1] Over the last decade, many surfaces have been developed for MEF based on different metallic nanoparticles, such as those comprised of silver nanoparticles,[2,3] gold colloids,[4] and even copper particulate films.[5] Several modes of silver deposition have also been developed, such as by wet chemistry,[6] a layer-by-layer deposition technique,[7] deposition by light,[8] electrochemically,[9] on glass,[10] plastic substrates,[11] and even on indium tin oxide.[12]

In addition, the value of MEF as a powerful platform technology for surface assays has been demonstrated for fluorescence-based applications of drug discovery[2] high-throughput screening,[13] immunoassays[14] and protein–protein detection.[15] In all these applications of MEF, the excitation and emission observations have been on the same side of the assay platform as the incoming excitation. It is well known that when fluorophores are near interfaces with different refractive indices (such as air and glass), a significant part of the fluorescence can be coupled into the medium of higher refractive index,[16] with a unique angular dependence peaking at the critical angle.[17] Moreover, the fluorescence emission through the high refractive index medium (and in air) could further be increased, when metallic nanoparticles are placed between the fluorophores and the interface. This phenomenon arises from the fact that metallic nanoparticles (especially silver, gold and copper) are known to scatter light efficiently and in an angular-dependent fashion.[18] In fact, 30 nm silver nanoparticles scatter light (at 530 nm) *ca.* 9 and 124 times more efficiently than 30 nm gold and polystyrene nanoparticles, respectively.[18] Subsequently, light scattering by silver and gold nanoparticles can be detected at concentrations as low as 10^{-16} M.[18] It was previously shown that scattered light by metallic nanoparticles is highest at observation angles of 0 and 180° with respect to the incident light, *i.e.* backward and forward scatter. Thus, when silver (also gold or copper) nanoparticles are placed between the fluorophores and the interface (glass

Institute of Fluorescence, Laboratory for Advanced Medical Plasmonics and Laboratory for Advanced Fluorescence Spectroscopy, Medical Biotechnology Center, University of Maryland Biotechnology Institute, 725 West Lombard St., Baltimore, MD, 21201, USA.
E-mail: geddes@umbi.umd.edu

† Electronic supplementary information (ESI) available: TEM images of silver colloids and angular-ratiometric intensity measurement results. See DOI: 10.1039/b709170b

‡ The HTML version of this article has been enhanced with colour images.

substrate), coupled light originated from the fluorophore will be preferentially scattered in backward and forward directions by the silver nanoparticles. The forward scattered light then couples to glass and is subsequently emitted from the back of the glass substrate, while the backward scattered light is emitted into free space. In addition, the angular-dependent scattered light from metallic nanoparticles depends on the size, shape and composition of the nanoparticles, as well as on the refractive index of the suspending medium, and is significantly different from the light scattered by planar glass.[18]

Many examples of assays based on the absorption (of light) properties of nanoparticles[19–29] as well as many examples of assays (solution or surface) utilizing the scattering properties of noble metallic nanoparticles can be found in the literature.[4,30–33] However, these assays do not combine the fluorescence and coupled scattered fluorescence properties which would be very beneficial for surface assays. One can find several reports in the literature pertaining to angular-dependent enhanced fluorescence by metallic nanoparticles, which offer a somewhat basic understanding based on simple observations from fluorophores placed in close proximity to these highly efficient light scattering nanoparticles: for example, Kawasaki and Mine[34,35] recently reported that highly reflective silver island films (60–200 nm width and 30–60 nm thick) grown on mica resulted in an enhanced emission from rhodamine dyes, with a greater part of the enhanced fluorescence emitted into the back half space through the silver island films and the mica substrate. Our laboratories have also recently reported the observation of angular-dependent enhanced fluorescence from fluorophores near large gold colloids (40–200 nm in diameter) bound to glass substrates.[4] These observations[4,34] were explained by the Radiating Plasmon Model (RPM),[10,36] which is contained within the Unified Plasmon-Fluorophore Theory (UPFT), first postulated by Geddes and co-workers,[37] whereby the unified system, composed of the fluorophore and the metal colloids, emits with the spectral characteristics of the fluorophore, after the excitation and the partial radiationless energy transfer between the excited states of the fluorophore and the surface plasmons of the metallic particles. This interpretation of MEF has been facilitated by the previous findings of surface-plasmon field-enhanced fluorescence spectroscopy[38] whereby fluorophores distal to a continuous metallic film can directionally radiate fluorophore emission at a unique angle from the back of the film. Remarkably, the plasmon-coupled emission is nearly completely p-polarized, irrespective of the excitation polarization,[39] strongly indicating like MEF, that the emission is indeed coupled through the surface plasmons.

In this paper, we present our detailed findings on angular-dependent metal-enhanced fluorescence from a monolayer of fluorophore-labeled protein on silver colloids deposited onto glass substrates. We have studied the effect of silver colloid loading, and the angle of excitation and polarization on the angular-dependent MEF phenomenon. Finally, we demonstrate the application of angular-dependent MEF for angular-ratiometric surface assays, a new approach to high-sensitivity detection based on the ratiometric response of MEF emission at two different angles. The emission at 225° (I_{225}) increases as a function of surface assay protein loading, while the enhanced emission at 340° (I_{340}) increases only modestly. Subsequently, a near-linear relationship between I_{225}/I_{340} *versus* concentration of surface protein can be realized, which is independent of the surface loading of silver, concentration of fluorophore used and fluctuations in background ambient and excitation light.

Experimental

Materials

Bovine-biotinamidocaproyl-labeled albumin (biotinlyated-BSA), fluorescein isothiocyanate (FITC)-labeled human serum albumin (FITC-HSA), silver nitrate (99.9%), trisodium citrate, and premium quality aminopropylsilane (APS)-coated glass slides (75 × 25 mm) were obtained from Sigma-Aldrich. FITC-labeled avidin was obtained from Molecular Probes (Eugene, OR). All chemicals were used as received.

Methods

Synthesis of silver colloids. The synthesis of silver colloids was performed using the following procedure as described previously:[10] 2 ml of 1.16 mM trisodium citrate solution was added drop-wise to a heated (90 °C) 98 ml aqueous solution of 0.65 mM of silver nitrate while stirring. The mixture was kept heated for 10 min, and then it was cooled in ice until use. This procedure yields 40 nm silver colloids as confirmed by TEM analysis (see ESI,† Fig. S1).

Deposition of silver colloids onto APS-coated glass substrates. The deposition of the silver colloids onto APS-coated glass slides was achieved by incubating the glass slides in a freshly prepared solution of silver colloids for 30 min, 2 h and overnight for the samples of OD = 0.075, 0.150 and 0.420, respectively. The APS-coated glass slides were coated with silver colloids due to the binding of silver to the amine groups' amine-terminated silane groups as demonstrated previously by our laboratories.[40] The other half of the glass slides were left intentionally blank for the control experiments. The silver colloid-deposited glass slides were rinsed with deionized water several times prior to the fluorescence experiments.

Absorption, angular-dependent light scattering, angular-dependent fluorescence measurements on silver colloids and on glass. All absorption measurements were performed using a Varian Cary 50 UV-Vis spectrophotometer.

The angular-dependent light scattering from glass and silver colloids was measured using an *X*–*Y* rotating stage (Edmund Optics) that was modified to hold a glass slide, with a fiber optic mount (Fig. 1). The glass and silver colloids were illuminated with a polarized laser source, the second harmonic (473 nm) of the diode-pumped Nd:YVO_4 laser (compact laser pointer design, output power *ca.* 30 mW), at an angle of 45 and 90° (from the surface of the glass substrate), and a neutral density filter was used to attenuate the laser intensity. The angular-dependent polarized scattered light at 473 nm from the silver colloids was collected through a dichroic sheet polarizer (Edmund Optics) into a 600 micron broad wavelength fiber that was connected to an Ocean Optics HD2000 spectrofluorometer. It is important to note that the polarizer

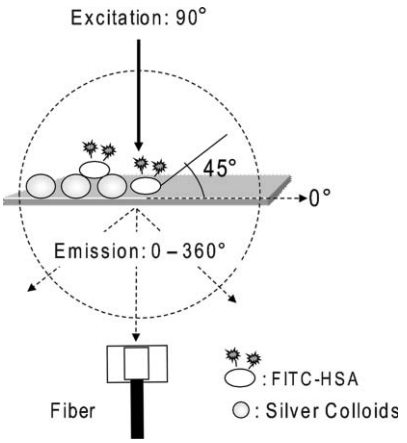

Fig. 1 Experimental setup.

was placed in front of the fiber (detector) during all measurements. The polarizations in the light scattering measurements are: excitation–emission: 1: p–p, 2: p–s, 3: p–(p + s) no polarization.

Binding the FITC-HSA to the silver colloids and to the glass surfaces was accomplished by incubating a 35 μl solution of 10 μM FITC-HSA on silver colloids and on glass for 30 min, followed by rinsing with PBS buffer to remove the unbound material. Both the silver colloids and glass surfaces were coated with FITC-HSA, which is known to passively absorb to noble metal surfaces and to form a *ca.* 4 nm thick protein monolayer, allowing us to study the fluorescence spectral properties of non-covalent FITC-HSA complexes in the absence and presence of silver colloids. By equally coating the surfaces with FITC-HSA we were also able to determine the enhancement factor (benefit) obtained from using the silver, *i.e.* intensity on silver/intensity on glass, given that both surfaces are known to have an approximately equal monolayer coverage.

The model assay used in this paper is based on the well-known interactions of biotin and avidin. Biotin groups are introduced to the surface through biotinlyated-BSA, which, similar to HSA, readily forms a monolayer on the surface of silver colloid films.[41–43] Binding the biotinlyated-BSA to the silver colloid-modified and unmodified part of glass slides was accomplished by incubating 10 μM biotinlyated-BSA solution on the surfaces for one hour, followed by rinsing with water to remove the unbound material. For the model assay, then 35 μl of 10–4500 nM FITC-labeled avidin was subsequently added to the biotinlyated-BSA-coated surfaces for 30 min, followed by rinsing with PBS buffer to remove the unbound material.

Angular-dependent fluorescence spectra of FITC-HSA and FITC-avidin in the model assay on glass and silver colloids were collected in a *similar* fashion to light scattering measurements, where the excitation light was eliminated with an emission filter at 488 nm. The angular-dependent fluorescence emission peak of FITC-HSA and of FITC-avidin were recorded at 517 nm. The polarization in the fluorescence measurements are: excitation–emission: 1: p–p.

The real-color photographs of FITC-HSA on silver colloids and glass slides were taken with a Canon digital camera (3.2 Mega Pixel, 10× optical zoom) using the same long-pass filter that was used for the emission spectra.

Results and discussion

It has previously been shown that the fluorescence emission from fluorophores in close proximity to silver nanoparticles is increased as the loading of silver nanoparticles on a glass substrate is increased.[44,45] Moreover, in our publications on MEF to date, the maximum amount of fluorescence enhancement was observed when the optical density (OD) of the silver nanoparticles was *ca.* 0.4.[2] Since MEF is related to the surface plasmons' ability to scatter the fluorophore's coupled excited-state energy, according to the UPFT,[37] we deemed it prudent to question the effect of silver colloid loading on the angular-dependent scattering of light by colloids. In this regard, glass surfaces with three different extents of silver colloid loading were prepared: OD = 0.075, 0.150 and 0.420 (for the sake of simplicity, these surfaces will be referred to as *low*, *medium* and *high* loading from this point on, respectively). Fig. 2 shows the absorption spectra of these surfaces. The surface plasmon resonance (SPR) peak for silver colloids on glass slides appears around 405 nm for surfaces with low and medium loadings, and 415 nm for surfaces with high loading. The surfaces with high loading show a slight red-shift in the SPR peak (as expected) due the reduction in the distances between the individual colloids which results in coupling of the surface plasmons, but not due to aggregation of silver colloids on the surface.

The evaluation of any metallic surfaces for MEF capability is undertaken by comparing the measured fluorescence intensity to a control sample substrate that does not contain the metallic nanoparticles. In this regard, angular-dependent light scattering by glass (the control substrate) was measured as shown in Fig. 3(top). When the glass surface is illuminated at 90°, p-polarized excitation source (473 nm laser), one can see that the scattered light is mostly p-polarized and biased parallel towards the angle of incident light.

Similar directional and polarization bias can be observed when the excitation angle is 45° [see ESI,† Fig. S2 (Top-Left)]. Further, the intensity of scattered light in the forward direction (from the back side of glass) was always observed to be greater

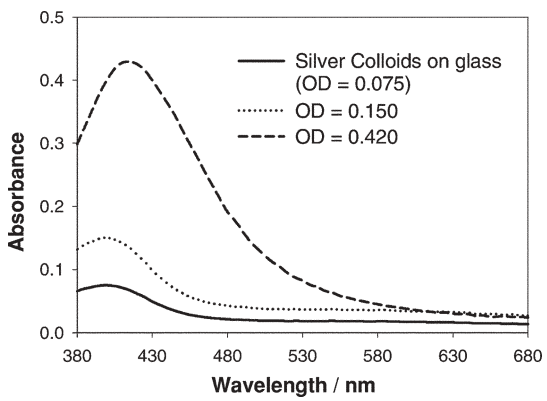

Fig. 2 Absorption spectra of silver colloids deposited onto glass slides.

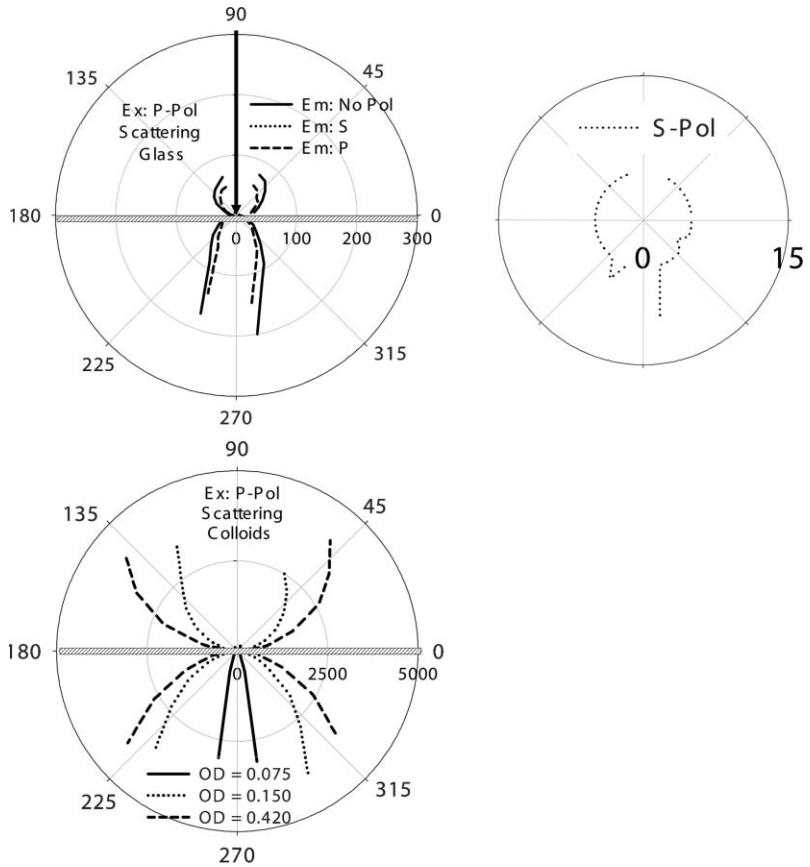

Fig. 3 Angular-dependent scattered light from glass (top) and silver colloids with different loading density (bottom). The inset (top-right) shows the s-polarized emission from glass. The p-polarized excitation was at 473 nm and at an angle of 90°. Ex: Excitation. Em: Emission, and represents the scattered light detected. No Pol: no polarizer. Intensity values for angles between 50 and 120° and for 270 ± 30° were not measured due to experimental setup constraints and due to saturation of the detector, respectively.

than the intensity in the back direction. Similar observations have also been made by Kawasaki and Mine[35] (only for the 90° excitation angle), and can be explained by Lambert's cosine law, assuming that glass is a Lambertian surface. The Lambert cosine law states that the intensity of scattered light, $I(\phi)$, at an angle ϕ from the normal to the surface, is represented by[35]

$$I(\phi) = I_0\cos\phi \qquad (0 \leqslant \phi \leqslant \pi/2) \tag{1}$$

Similarly, the angular-dependent scattered intensity from the back of the glass, $I_2(\phi)$, is governed by[35]

$$I_2(\phi) = \left(\frac{1}{n_2^2}\right) I_0 |\cos\phi| \qquad (\pi/2 \leq \phi \leq \pi) \tag{2}$$

where n_2 is the refractive index of the glass. According to eqn (2), the light initially scattered into the glass also follows the cosine law but was 2.28 (square of n_2 = 1.51) times larger than the intensity detected in the backspace.

Given that the scattered light from glass is mostly polarization-dependent, then only p-polarized, angular-dependent light scattering from silver colloid-deposited glass substrates with different loading densities were measured as shown in Fig. 3(bottom). When the silver colloid-deposited surfaces were illuminated by the same p-polarized source, one can see that the scattered light from silvered surfaces with low loading density follows a similar angular dependence as the glass substrate. On the other hand, as the loading of silver nanoparticles is increased (medium and high loadings), the forward and backward scattered intensities had similar values, and were observed at much wider angles. Intensity measurements for angles between 50 and 120° and at 270 ± 30° were not possible due to experimental setup constraints and to saturation of the detector, respectively.

The scattering of light by sub-wavelength metallic nanoparticles themselves can be described by Rayleigh theory[46] [according to Yguerabide and Yguerabide,[18] nanoparticles up to 40 nm are considered to be in the Rayleigh limit, and we assume that the silver colloids (40 nm) used in this study can also be approximately considered within this category]. For incident polarized light, the intensity of angular-dependent light scattered, I_{scatt}, in the direction θ (angle) by a homogeneous spherical particle with radius $a \ll \lambda$ (wavelength) of the incident beam is also polarized and can be described as given by the Rayleigh expression[18,46]

$$I_{\text{scatt}} = \frac{16\pi^4 a^6 n_{\text{med}}^4 I_0}{r^2\lambda^4}\left|\frac{m^2-1}{m^2+2}\right|\cos^2\theta \tag{3}$$

where I_0 is the incident intensity of monochromatic light, n_{med} is the refractive index surrounding the particle, m is the refractive index of the bulk particle material (both functions of

the incident wavelength) and r is the distance between the particles.

Interestingly, from eqn (3), the scattered light intensity is highest at the observation angles $\theta = 0$ and 180° (backward and forward angles), is zero at $\theta = 90$ and 270°, the intensity being proportional to $\cos^2\theta$. It is important to note that these angles are defined with respect to the *direction of the incident light* and are rotated by 90° in our experimental system, therefore these angles correspond to $\theta = 90°$ (backward), 270° (forward), 180° and 360° in our data (alternatively, one can assign the angle of incident light as 0° and change the angle designations in Fig. 2). A close examination of eqn (3) also reveals that as the distance between the particles (r) decreases, the intensity of the scattered light increases. One can decrease r by increasing the loading of the nanoparticles on the surface, as is done in this study. Therefore, our observations in Fig. 3(bottom), where the forward and backward scattered intensities had similar values and increased as the loading of silver is increased, is in agreement with eqn (3). In addition, the fact that by increasing the loading of silver nanoparticles up to a level optimized for MEF (OD = 0.4, high loading), the scattered light can be observed at much wider angles affords for measurements to be undertaken at different angles for angular-ratiometric assays (described later). We note that several factors play an important role in the angular-dependent scattering of light: (1) multiple scattering events: scattered light from a nanoparticle is reflected by another silver nanoparticle before scattering into the surrounding medium; (2) broader surface plasmon bands: as the loading of silver nanoparticles increases, nanoparticle resonances couple, effectively scattering light like larger nanoparticles;[30] (3) refractive index of the supporting substrate; (4) excitation angle.

The angular-ratiometric intensity measurements described later offer many advantages over single intensity measurements. More specifically, angular-ratiometric measurements are (i) independent of the total light intensity and are therefore not perturbed by excitation source instabilities or drifts, and (ii) can be performed at a variety of angles offering multiple readout choices for the user. It should be also noted that a similar discussion also applies for coupled scattered light when a 45° excitation angle is used (see ESI,† Fig. S2).

It is well known that for fluorophores near interfaces with different refractive indices (such as air and glass), a significant part of the fluorescence can be coupled into the medium of higher refractive index,[16] with a unique angular dependence peaking at the critical angle.[17] Given that MEF is related to the surface plasmons' ability to scatter the coupled emission, we questioned whether or not the fluorescence emission through the high refractive index medium can be further increased (enhanced emission) but also in an angular-dependent fashion, when metallic nanoparticles are placed between the fluorophores and the glass interface. For comparison, we have also studied the angular-dependent emission from fluorophores on glass (a control sample). In this regard, first, a monolayer of fluorophore (FITC)-labeled HSA was deposited onto surfaces with silver colloids and onto a control sample (*unsilvered* glass). Fig. 4 shows the polarized emission intensity (polar plots) of FITC-HSA from glass substrates and on silver colloids with different loadings,

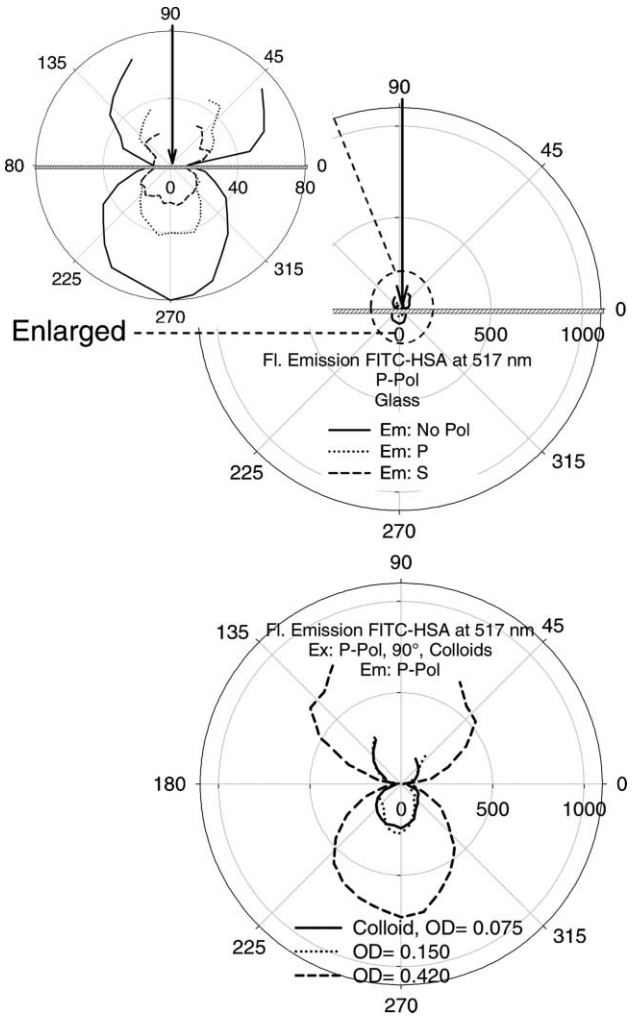

Fig. 4 Angular-dependent p-polarized fluorescence emission intensity (measured at 517 nm) for FITC-HSA on glass (top) and silver colloids (bottom). Excitation was p-polarized and was at an angle of 90° to the surface.

measured at 517 nm in an angular-dependent fashion, *i.e.* over 360°. The excitation source was positioned perpendicular to the glass substrate, and was on the same side as the silver colloids and the fluorophores. The emission intensities between the angles of 70 and 110° were not collected due to the obstruction by the fiber optic holder as explained earlier in the experimental section. The emission intensity of FITC-HSA on glass and silver colloids was the weakest at the angles of 0° (equivalent to 360°) and 180°, and was the highest at 270° (at the back of the glass substrates). The emission intensity at all angles was higher on silver colloids with a high loading than with a medium loading and low loading respectively. In addition, the emission intensity at all angles was higher on silver colloids than on glass, which we attribute to MEF. Similar observations were also made from the same surfaces when the excitation angle employed was 45° (see ESI†).

Fig. 5 shows the p-polarized emission spectra (p–p) of FITC-HSA on glass and silver colloids (low loading) observed at four different observation angles: 45, 135, 225 and 315°. The emission spectra shown here are typical of those of FITC

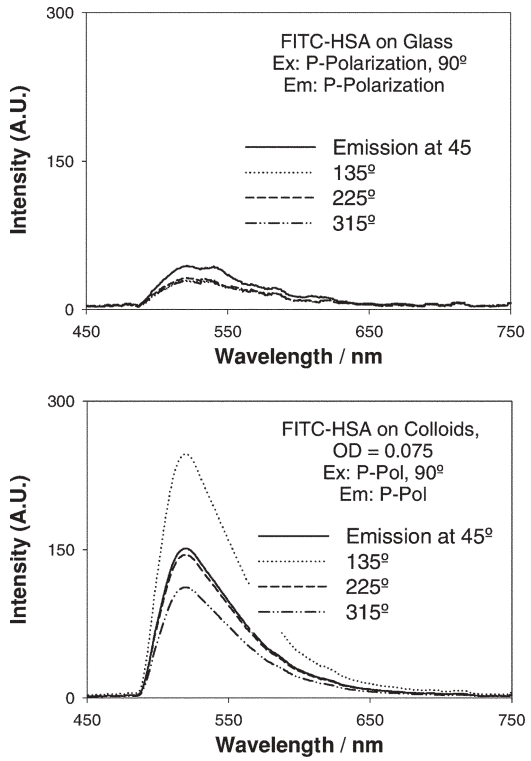

Fig. 5 The p-polarized emission spectra of FITC-HSA on glass (top) and silver colloids (bottom) observed at 45, 135, 225 and 315°. Excitation source was p-polarized and was positioned at an angle of 90°. A.U.: arbitrary units.

measured on glass substrates,[47] and have a maximum emission peak of 517 nm. The emission intensity of FITC at 517 nm is the largest for silver colloids as compared to glass at all angles, and was the largest at an observation angle of 270° for the silver colloids data, Fig. 4(bottom).

Fig. 6 provides a visual demonstration for the enhancement of fluorescence emission by the MEF effect, for FITC-HSA on silver colloids with respect to that of on glass, where the real-color photographs of fluorescence emission on glass and on silver colloids (low loading) were taken at observation angles of 225 and 315° through an emission filter. The fluorescence emission on silver colloids at both angles is much brighter than that of the glass substrate. Fig. 6 also shows that the shape of the normalized emission spectra of FITC-HSA on both glass and silver colloids *are almost identical* at observation angles of 225 and 315°, showing that little spectral change for FITC occurred when coupled to silver colloids, *i.e.* MEF. A closer inspection of the spectra in Fig. 6(bottom) does, however, show that the MEF spectra at both 225 and 315° are slightly narrower than the fluorescence emission observed from glass. These observations were common for all coupled angles, and while this observation in not fully understood today, it is a question in ongoing studies in our laboratory.

In order to interpret the observed angular-dependent metal-enhanced fluorescence shown in Fig. 4 in a *quantitative manner*, MEF enhancement factors [emission intensity at 517 nm (I_{517}) on silver colloids divided by I_{517} on glass] were calculated at all observation angles and are shown in Fig. 7 (see also ESI,† Fig. S4). MEF enhancement factors of 3–4 and 7–9 can be seen for FITC emission on silver colloids with low and medium loadings, and high loading, respectively. One can see that when silver colloids were present between the fluorophores and the interface, the fluorescence emission from the air and back side, increased to a similar extent. Clearly, the enhanced fluorescence was significantly greater from surfaces with a higher degree of colloid loading (OD = 0.4).

Fluorophore detectability is a major factor that governs the utility and sensitivity of fluorescence-based sensing approaches.[48] It is widely accepted that the detectability of a fluorophore is primarily determined by three factors: the extent of background emission from the sample, the quantum yield, and the photostability of the fluorophore.[48] Given that the scattering of light and enhancement of fluorescence by silver colloids varies with the angle of observation, we subsequently questioned whether the photostability of FITC would also vary with the angle of observation, noting that MEF affords for reduced fluorophore lifetimes[40,49] also in addition to enhanced emission intensities. Subsequently, the photostability of FITC-HSA on glass and silver colloids (with three different loadings) was measured at two different angles, 225 and 340°. Fig. 8 shows the FITC emission intensity at 517 nm as a function of time, when excited at 473 nm and observed through a 488 nm razor-edge filter. The relative intensities within the plots indicate that a higher photon flux can be observed from the silver colloids at 225°, as compared to 340° and also as compared to glass at both angles. Since the integrated areas under the plots are proportional to the photon flux from the respective samples, one can see that FITC is more photostable on silver colloids at 225°, after adjusting the laser power to match the same *initial steady-state intensities* of FITC on glass and silver colloids, Fig. 8. Interestingly, the angular-dependent photostability suggests that the observed enhanced emission is not solely due to coupling through glass, but is indeed a part result of directional MEF as well, which is thought to be governed by the scattering properties of the particles. In MEF, the fluorescence emission is enhanced, while the lifetime of the fluorophores is typically reduced.[2] The increased photostability at different angles suggests also that the lifetime of the FITC is shorter at 225° (not measured here due to difficulties that such measurements pose), the FITC in essence spending less time, on average, in an excited state due to the fast radiationless energy transfer to the induced metal plasmons, and is therefore less prone to photodegradation, *i.e.* is more photostable. As expected for the glass control samples, the photostability and therefore probably lifetime also, do not show a noticeable angular dependence, Fig. 8(bottom-right).

It is important to discuss the factors affecting the angular-dependent and enhanced emission observed in this work. At present, the angular-dependent enhanced fluorescence emission is attributed to the following factors:

(1) silver colloids: simple MEF effect creating enhanced emission, and reduced lifetime yielding enhanced photostability;

(2) the loading of silver colloids on the surface: as the loading (measured by OD) increases, the particle plasmons couple, producing more forward scatter, analogous to Mie theory for larger particles; subsequently, plasmon-coupled

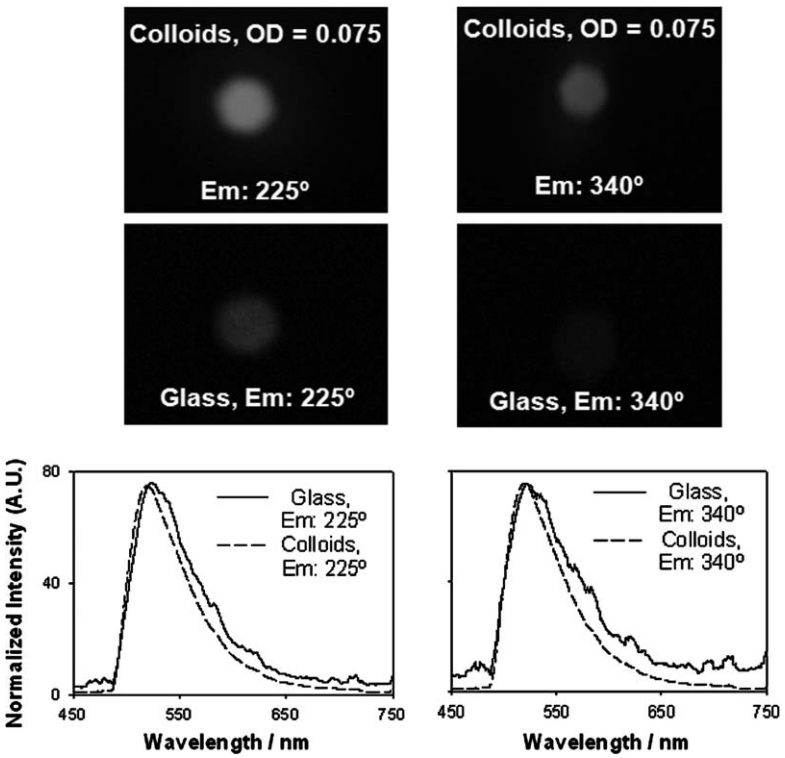

Fig. 6 Real-color photographs of fluorescence emission of FITC-HSA on glass and silver colloids taken through an emission filter (488 nm) at 225 and 340° (top). Normalized emission spectra of FITC-HSA on glass and silver colloids measured at the same angles (bottom).

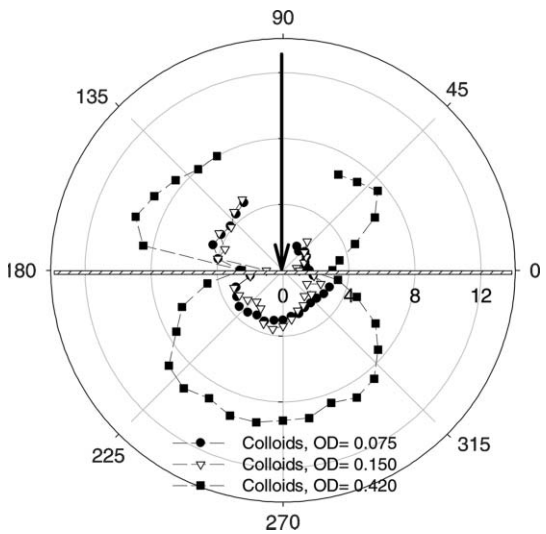

Fig. 7 Angular-dependent metal-enhanced fluorescence (MEF) *enhancement factor* [emission intensity at 517 nm (I_{517}) on silver colloids divided by I_{517} on glass (control sample) for all angles]. Fluorescence emission intensity was measured through a 488 nm razor-edge filter.

fluorescence shows an increased forward intensity distribution and enhanced emission intensities;

(3) the angle of initial excitation (creates bias in the direction of emission), *i.e.* Mie forward scatter (see also ESI,† Fig. S2–S4);

(4) glass substrate provides for cos θ dependence coupling;

(5) fluorophore labeling: the fluorophore is thought to be located both on the glass and silver colloids, hence the intensity distribution of the plasmon-coupled fluorescence (MEF) does not exactly follow the scattering of light by the colloids themselves.

The angular-dependent enhanced fluorescence emission from silver colloid-deposited surfaces shown in Fig. 4 roughly follows the angular-dependent light scattering pattern by the silver colloids. That is, the increased fluorescence emission can be observed at wider angles (towards 0 and 180°), where light scattering by silver colloids on the glass substrate (especially by high loading) is increased. This can be explained by the Rayleigh expression, whereby when the distance between the colloids is decreased the intensity of scattered light subsequently increases and can be observed at wider angles. Moreover, when the loading of silver on the glass surface was low, the fluorescence emission through the surface can be observed at narrower angles, similar to fluorescence emission through an unsilvered glass surface. In fact, one can see that the light scattering directionality values for an unsilvered glass and glass surface with a low loading of silver colloids are very similar, providing evidence for the influence of silver colloids on the angular-dependent emission, and for MEF as a function of colloid loading. As the loading of silver colloids is increased on the surface, that is the distance between the colloids is reduced, the electric field contribution between the colloids is increased in addition to increased light scattering by colloids, contributing to the increased fluorescence emission both from the front and the back sides of these surfaces.

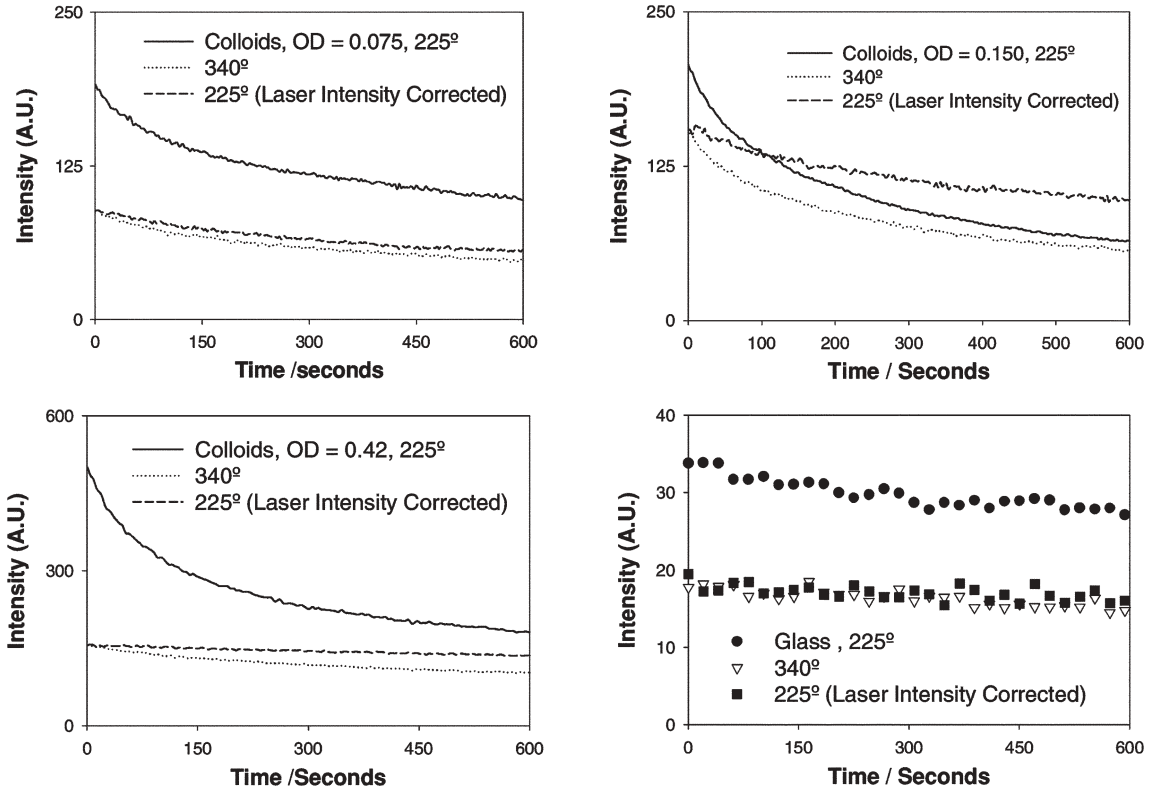

Fig. 8 Photostability of FITC-HSA from glass and silver colloids with OD = 0.075 (low loading), 0.150 (medium loading) and 0.420 (high loading). Excitation light was at an angle of 90°. Emission intensity (p-polarized) was measured at 517 nm and collected at 225 and 340°.

It was also found that the initial angle of incidence affected the angular-dependent pattern of the coupled-fluorescence emission. When the excitation angle was changed to 45°, both the light scattering and coupled-fluorescence from silvered surfaces were predominantly in the path of the incident light, *i.e.* the forward direction. Similar to scattered light from incident light at 90°, glass surfaces scattered light at narrow angles (still conforming to Lambert's cosine law), while the scattering of light from silvered surfaces can be observed at much wider angles. It is important to note that while it seems redundant to study angular-dependent MEF using two different angles, we believe that the results of this study might well offer a reference for fluorescence researchers whom use 45 and 90° excitation angles routinely on planar surfaces.

Angular-dependent MEF: opportunity for angular-ratiometric surface assays

To demonstrate the analytical utility of angular-dependent MEF for angular-ratiometric surface assays, we have constructed a model protein assay on silver colloid-deposited glass substrates, Fig. 9(top). Our model assay consisted of biotinlyated-BSA, which forms a monolayer on silver colloids[41,42] and positions fluorophores *ca.* 4 nm from silver colloids (an ideal distance for MEF[50]) and a fluorophore-labeled avidin. This model protein assay affords for simple kinetics without back-reactions due to the well-known strong association of biotin and avidin.[41,42]

In our system, since the fluorescence emission intensities from the back of the silver colloid-deposited glass substrates are easy to measure, and offer a range of observation angles to choose from (Fig. 4), we have chosen two observation angles, 225 and 340°, to monitor our model assay. Moreover, as shown in Fig. 4(bottom), the intensity at 225° is approximately three-fold larger than that measured at 340°, potentially further increasing the detectability of the fluorescence emission. A detailed examination of Fig. 4(bottom) reveals that even larger ratios of emission intensities can be achieved at 270 and 340° instead of our angles of choice. However, it should be noted that 270° is in the direct path of the scattered excitation light, and, thus, the fluorescence emission measurements at this angle require better detection filters (which increases the cost of the detection system) to completely eliminate the excitation light. Instead, we opted to use an 'off-axis' angle (225°) that does not necessarily require the use of expensive notch filters. It is also important to note that one can choose virtually any observation angle between 0 and 360° (except the angles obstructed by the excitation light) considering certain parameters such as detectable signal, experimental setup constraints and the costs of the associated filters.

Fig. 9 shows the fluorescence emission spectra of FITC-avidin on silver colloids (high loading) measured at 225 and 340° as a function of concentration. One can see that the emission intensities (at 517 nm) for all FITC-avidin concentrations measured at 225° are approximately three-fold larger than those measured at 340°, as also seen in Fig. 4(bottom). When the concentration-dependent emission intensity of FITC-avidin at 517 nm measured at 225 and 340° is plotted in a semi-logarithmic manner [Fig. 10(top)], it reveals that the

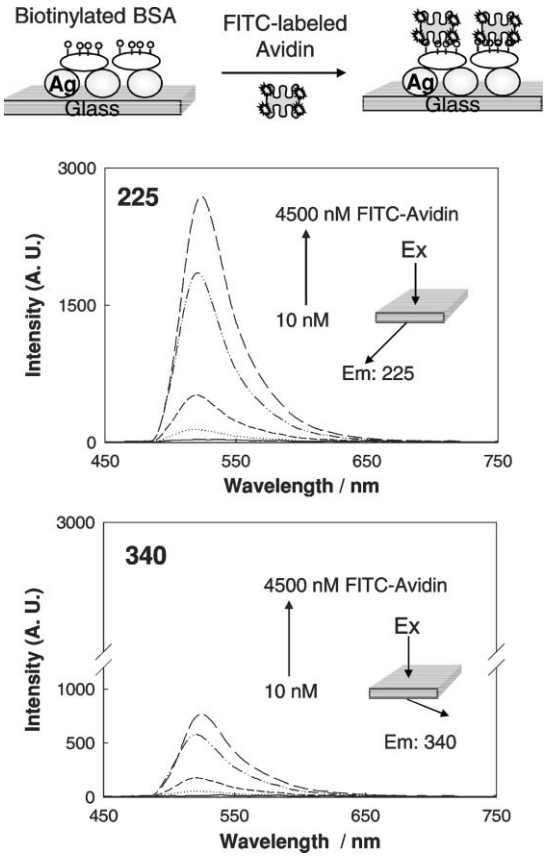

Fig. 9 Model angular-ratiometric MEF assay (top scheme). Fluorescence emission spectra of FITC-avidin on silver colloids (high loading) measured at 225 and 340° (bottom). Insets: schematic of excitation (Ex) and observation (Em) angles.

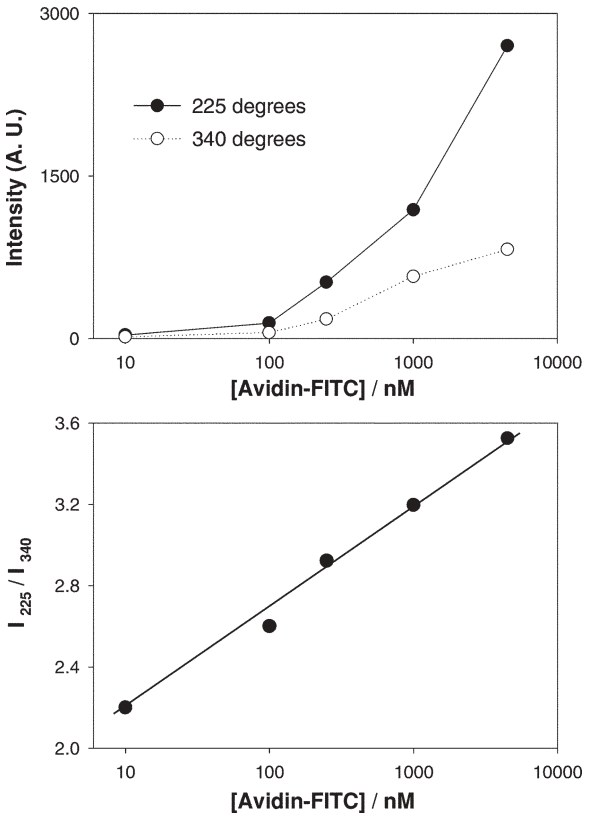

Fig. 10 Semi-logarithmic concentration-dependent plot of emission intensity of FITC-avidin at 517 nm measured at 225 and 340° (top) and angular-ratiometric (I_{225}/I_{340}) response obtained for the model MEF assay (bottom).

lower detection limit for FITC-avidin is less than 100 nM. On the other hand, when the *ratios* of emission intensities at 225 and 340° are plotted *versus* the concentration of FITC-avidin, the true effectiveness of an angular-ratiometric measurement is revealed [Fig. 10(bottom)]: the lower detection limit appears to be 10 nM, which cannot be clearly determined from the single-angle intensity measurements. Hence, by simply incorporating angular-ratiometric measurements, one can envisage a broader detection range and a potentially lower detection limit (*i.e.* accurate extrapolation) for MEF-based surface assays. It is important to note that the ratiometric intensity measurements here are independent of initial intensity and fluctuations in the excitation light, colloidal loading and also the loading of the fluorophore. Thus, angular-ratiometric measurements combined with the use of more sensitive detectors should further enhance the capability of MEF-based surface assays.

Conclusions

In this paper, we report our detailed studies on the angular-dependent metal-enhanced fluorescence from fluorophores in close proximity to silver colloids. Three different silvered surfaces were prepared *via* the deposition of silver colloids, *ca.* 40 nm in diameter, onto glass substrates in a homogenous manner as characterized by absorption spectroscopy. Initially, the angular-dependent light scattering properties of these three silvered surfaces and a control glass substrate were studied. The angular-dependent scattered light from glass surfaces was found to be dependent on polarization and angle of the incident light, and is readily explained by Lambert's cosine law. The intensity of scattered light in the forward direction (from the back side of glass) was found to be larger than the back-scattered intensity. On the other hand, the forward and backward scattered intensities from silvered surfaces had similar values and increased as the loading of silver was increased, and to some extent can be explained by Rayleigh–Mie expressions. In addition, the scattered light from the silvered surfaces was observed at much wider angles, which afforded for measurements to be undertaken at different angles for angular-ratiometric assays.

The angular-dependent fluorescence emission from fluorophores placed near to silver colloid-deposited glass surfaces was also investigated. It was observed that the fluorescence emission through silvered glass was increased in an angular-dependent fashion, following loosely the angular-dependent light scattering pattern produced by the silver colloids themselves. Similar observations for fluorescence emission from fluorophores deposited onto glass surfaces were made, but with much narrower angular distributions at both sides of the fluorophore–glass interface. As the loading of silver on glass was increased, the increased fluorescence emission was also observed at wider angles (towards 0 and 180°) from both sides of the silvered surfaces. In addition, the initial angle of

the excitation light biased the angular-dependent pattern of the fluorescence emission. This is an important observation which further supports MEF models described by Geddes and co-workers,[10,37] which suggests that it is the fluorophore-induced plasmon which radiates and not the fluorophore alone.

Finally, we have demonstrated the utility of the angular-dependent MEF phenomenon for intensity-based angular-ratiometric surface assays. A model protein assay on silvered surfaces was constructed, and the concentration-dependent fluorescence emission was measured at 225 and 340°. The angular-ratiometric MEF-based method afforded a linear response with respect to an increased concentration of the protein of interest with a lower detection limit of *ca.* 10 nM. We envisage broad applicability for our angular-ratiometric MEF method to many fluorescence-based surface assays.

Acknowledgements

This work was supported by the Middle Atlantic Regional Center of Excellence for Biodefense and Emerging Infectious Diseases Research (NIH NIAID – U54 AI057168). Salary support to authors from UMBI/MBC and the IoF is also acknowledged.

References

1 C. D. Geddes and J. R. Lakowicz, *J. Fluoresc.*, 2002, **12**, 121–129.
2 K. Aslan, I. Gryczynski, J. Malicka, E. Matveeva, J. R. Lakowicz and C. D. Geddes, *Curr. Opin. Biotechnol.*, 2005, **16**, 55–62.
3 Y. Chen, K. Munechika and D. S. Ginger, *Nano Lett.*, 2007, **7**, 690–696.
4 K. Aslan, S. N. Malyn and C. D. Geddes, *J. Fluoresc.*, 2007, **17**, 7–13.
5 Y. Zhang, K. Aslan, M. J. R. Previte and C. D. Geddes, *Appl. Phys. Lett.*, 2007, **90**, 173116.
6 K. Aslan, J. Huang, G. M. Wilson and C. D. Geddes, *J. Am. Chem. Soc.*, 2006, **128**, 4206–4207.
7 D. S. dos Santos and R. F. Aroca, *Analyst*, 2007, **132**, 450–454.
8 C. D. Geddes, A. Parfenov and J. R. Lakowicz, *Appl. Spectrosc.*, 2003, **57**, 526–531.
9 C. D. Geddes, A. Parfenov, D. Roll, J. Y. Fang and J. R. Lakowicz, *Langmuir*, 2003, **19**, 6236–6241.
10 K. Aslan, Z. Leonenko, J. R. Lakowicz and C. D. Geddes, *J. Fluoresc.*, 2005, **15**, 643–654.
11 K. Aslan, P. Holley and C. D. Geddes, *J. Mater. Chem.*, 2006, **16**, 2846–2852.
12 H. J. Park, D. Vak, Y. Y. Noh, B. Lim and D. Y. Kim, *Appl. Phys. Lett.*, 2007, **90**, 161107.
13 K. Aslan, P. Holley and C. D. Geddes, *J. Immunol. Met.*, 2006, **312**, 137–147.
14 K. Aslan and C. D. Geddes, *Plasmonics*, 2006, **1**, 53–59.
15 C. D. Geddes, K. Aslan, I. Gryczynski, J. Malicka and J. R. Lakowicz, in *Topics in Fluorescence Spectroscopy. Vol. 8: Radiative Decay Engineering*, ed. C. D. Geddes and J. R. Lakowicz, Kluwer Academic/Plenum Publishers, New York, 2005, ch. 14, pp. 405–448.
16 J. Enderlein, T. Ruckstuhl and S. Seeger, *Appl. Opt.*, 1999, **38**, 724–732.
17 J. I. Gersten and A. Nitzan, *Chem. Phys. Lett.*, 1984, **104**, 31–37.
18 J. Yguerabide and E. E. Yguerabide, *Anal. Biochem.*, 1998, **262**, 137–156.
19 K. Aslan and C. D. Geddes, *Anal. Chem.*, 2007, **79**, 2131–2136.
20 K. Aslan, J. R. Lakowicz and C. D. Geddes, *Anal. Chim. Acta*, 2004, **517**, 139–144.
21 K. Aslan, J. R. Lakowicz and C. D. Geddes, *Anal. Biochem.*, 2004, **330**, 145–155.
22 R. Elghanian, J. J. Storhoff, R. C. Mucic, R. L. Letsinger and C. A. Mirkin, *Science*, 1997, **277**, 1078–1081.
23 H. Li and L. Rothberg, *Proc. Natl. Acad. Sci. U. S. A.*, 2004, **101**, 14036–14039.
24 H. Li and L. J. Rothberg, *Anal. Chem.*, 2004, **76**, 5414–5417.
25 N. Nath and A. Chilkoti, *Anal. Chem.*, 2002, **74**, 504–509.
26 H. Wei, J. Li, Y. L. Wang and E. K. Wang, *Nanotechnology*, 2007, 18.
27 M. Sackmann, S. Bom, T. Balster and A. Materny, *J. Raman Spectrosc.*, 2007, **38**, 277–282.
28 K. Kneipp, H. Kneipp, I. Itzkan, R. R. Dasari and M. S. Feld, *Chem. Rev.*, 1999, **99**, 2957–2976.
29 N. Felidj, J. Aubard, G. Levi, J. R. Krenn, A. Hohenau, G. Schider, A. Leitner and F. R. Aussenegg, *Appl. Phys. Lett.*, 2003, **82**, 3095–3097.
30 K. Aslan, P. Holley, L. Davies, J. R. Lakowicz and C. D. Geddes, *J. Am. Chem. Soc.*, 2005, **127**, 12115–12121.
31 K. Aslan, J. R. Lakowicz and C. D. Geddes, *Appl. Phys. Lett.*, 2005, **87**, 234108.
32 K. Aslan, J. R. Lakowicz and C. D. Geddes, *Curr. Opin. Chem. Biol.*, 2005, **9**, 538–544.
33 K. Aslan, J. R. Lakowicz and C. D. Geddes, *Anal. Chem.*, 2005, **77**, 2007–2014.
34 M. Kawasaki and S. Mine, *J. Phys. Chem. B*, 2005, **109**, 17254–17261.
35 M. Kawasaki and S. Mine, *Chem. Lett.*, 2005, **34**, 1038–1039.
36 J. R. Lakowicz, *Anal. Biochem.*, 2005, **337**, 171–194.
37 K. Aslan, M. J. R. Previte, Y. X. Zhang and C. D. Geddes, *Biophys. J.*, 2007, 371A–371A.
38 T. Liebermann and W. Knoll, *Colloids Surf., A*, 2000, **171**, 115–130.
39 J. R. Lakowicz, *Anal. Biochem.*, 2004, **324**, 153–169.
40 K. Aslan and C. D. Geddes, *Anal. Chem.*, 2005, **77**, 8057–8067.
41 N. M. Green, *Adv. Protein Chem.*, 1975, **29**, 85–133.
42 M. Wilchek and E. A. Bayer, *Anal. Biochem.*, 1988, **171**, 1–32.
43 M. Wilchek and E. A. Bayer, *Methods Enzymol.*, 1990, **184**, 14–45.
44 J. R. Lakowicz, Y. B. Shen, S. D'Auria, J. Malicka, J. Y. Fang, Z. Gryczynski and I. Gryczynski, *Anal. Biochem.*, 2002, **301**, 261–277.
45 C. D. Geddes, H. Cao, I. Gryczynski, Z. Gryczynski, J. Fang and J. R. Lakowicz, *J. Phys. Chem. A*, 2003, **107**, 3443–3449.
46 M. Kerker, *The scattering of light and other electromagnetic radiation*, Academic Press, New York, 1969.
47 K. Aslan, R. Badugu, J. R. Lakowicz and C. D. Geddes, *J. Fluoresc.*, 2005, **15**, 99–104.
48 J. R. Lakowicz, *Principles of Fluorescence Spectroscopy*, Kluwer Academic, New York, 2nd edn, 1999.
49 K. Aslan, I. Gryczynski, J. Malicka, J. R. Lakowicz and C. D. Geddes, *Metal-Enhanced Fluorescence: Application to High-Throughput Screening and Drug Discovery*, ed. S. Gad, Wiley & Sons, New Jersey, 2005.
50 J. R. Lakowicz, *Anal. Biochem.*, 2001, **298**, 1–24.